# Simulations of ion transport in a collisional radio-frequency plasma sheath

Zhong-Ling Dai* and You-Nian Wang
*The State Key Laboratory of Materials Modification by Laser, Electron, and Ion Beams, Department of Physics, Dalian University of Technology, Dalian 116023, People's Republic of China*
(Received 10 November 2003; published 12 March 2004)

A hybrid theoretical model, capable of describing the characteristics of a collisional sheath driven by a sinusoidal current source and determining the energy and angular distributions of ions incident onto the substrate, is proposed. The model consists of one-dimensional time-dependent fluid equations coupled with the Poisson equation determining spatiotemporal evolution of the sheath and the Monte Carlo simulation predicting the energy and angular distributions of ions striking the electrode, in which charge-exchange collisions between ions and neutrals are included. Additionally, an equivalent circuit model in conjunction with the fluid equations is adopted to self-consistently determine the relationship between the instantaneous potential at a rf-biased electrode and the sheath thickness. It is found that the collisional effects would influence the height of the energy peaks in the ion energy distributions and the ion angular distributions.

DOI: 10.1103/PhysRevE.69.036403 PACS number(s): 52.65.−y, 52.40.Hf

## I. INTRODUCTION

In processing plasmas, it is well known that the ion energy and ion angular distributions (IEDs and IADs) arriving at the substrate are crucial in etching and deposition rates of the film as well as the surface topography evolution. In order to produce the desired anisotropic etching, an electrode on which the substrate is placed is usually biased independently by a radio-frequency (rf) power generator. The role of the bias is to yield a sheath electric field which accelerates the ions from the plasma toward the substrate surface. In general, the motion of the ions as well as the IEDs and IADs are determined by the spatiotemporal variations of the sheath electric field and the collisions the ions undergo while traversing the sheath.

To control anisotropic etching, some low-pressure (1–50 mTorr), high-density ($10^{11}$–$10^{12}$ cm$^{-3}$) plasma sources, such as inductively coupled plasma source, is often used in the plasma etching processes. In this case, due to the sheath thickness being much less than the ion mean free path, it is reasonable to neglect the collisional effects on the motion of ions in the sheath. Thus, the ions strike the surface with high energy and momentum concentrated in the direction normal to the surface. For the collisionless rf sheath, the characteristics of the sheath can be well described by the cold ion fluid model coupled with Poisson's equation [1–10]. In particular, it has been found both theoretically and experimentally [5,10–13] that, at low-pressure discharges, the IEDs are bimodal when the rf-biased source frequency is less than the ion plasma frequency.

In the field of film deposition, however, discharge pressures can be up to hundreds of mTorr, which would lead the ion mean free path close to the sheath thickness. Thus, one has to consider the collision effects on the motion of ions in the sheath. In recent years, significant progress has been achieved in studies of the characteristics of the collisional rf sheath using various approximate methods. In a subsequent work [14], Lieberman studied collisional effects on the rf sheath dynamics based on the step model, but the author assumed that the average ion potential energy gains from the rf electric field dissipate fully in the charge-exchange collisions between the ions and the neutral particles. However, such a collisional rf sheath model is only suitable to describe the sheath characteristics at very high-pressure discharges. An extended Lieberman's model [15,16] was proposed to describe the collisional rf sheath dynamics over a wide pressure range. It is found that the increase of the pressure can result in reduction of the ion bombardment energy and the thin of the sheath thickness. It should be stressed that all the time-dependent terms in the ion fluid equations were neglected in the above collisional sheath model, which is adequate only to extremely high rf sheath voltages or high bias frequencies.

In addition, the effects of the rf sheath collision processes on the IEDs and IADs have been simulated with the Monte Carlo method [17–20] which includes both the charge- and momentum-transfer collisions of ions with neutrals. In these simulations, however, some parametric models describing the sheath electric field were used to simulate the ion transport for reducing the costing in computation. The parameterized sheath electric field depends on the sheath thickness and the potential on the electrode. Recently, the spatiotemporal sheath electric field given by extended Lieberman's model was used in the Monte Carlo simulations [21].

Actually, when the bias frequency is less than or equal to the ion plasma frequency, one has to consider the time-dependent terms in the ion fluid equations. In this case, the motion of the ion is determined by the instantaneous sheath electric field, not the time-averaged field. For collisional rf sheaths, to the best of our knowledge, there were no studies reported on the sheath characteristics by including the time-dependent terms in the ion fluid equations. On the other hand, it is well known that, due to the effects of the sheath loading, the potential on the electrode is not exactly equal to the sinusoidal voltage supplied by the bias power. Thus, it is not suitable to simulate the ion trajectories in the rf sheath using the parametrized sheath electric field.

*Email address: daizhl@dlut.edu.cn

 ©2004 The American Physical Society

In this paper, we wish to use a hybrid model to study the characteristics of collisional sheaths. The hybrid model will include two parts: the dynamics model of the collisional rf sheath and the Monte Carlo model of the ion transport across the sheath. This paper is outlined as follows. In Sec. II the dynamic model of the collisional rf sheath is described by the ion fluid equations which includes all the time-dependent terms and an equivalent circuit model. Some numerical results of the amplitude of potential on the electrode and the average sheath thickness as well as the spatiotemporal variation of the electric field are also shown in the section. Then, in Sec. III, the spatiotemporal variation of the electric field is further used in the Monte Carlo simulation of the collisional ion transport across the sheath to determine the IEDs and IADs striking the substrates. Finally, a short summary is given in Sec. IV.

## II. DESCRIPTION OF SHEATH MODEL

We consider that a rf-bias power is applied to a planar electrode inside a plasma. Then, a rf sheath will be formed near the electrode surface where collisions in the sheath should be included. The plasma which consists of single charged ions and electrons is described by a two-fluid model. We may neglect the ion thermal motion effects since the ion temperature is much smaller than the directional kinetic energy in the sheath regions. In the following, a one-dimensional configuration, with the electrode placed at $x=0$, is adopted. Thus, the one-dimensional spatiotemporal variation of the ion density, $n_i(x,t)$, and the ion drift velocity, $u_i(x,t)$, are described by the cold ion fluid equations

$$\frac{\partial n_i}{\partial t}+\frac{\partial(n_i u_i)}{\partial x}=0, \tag{1}$$

$$\frac{\partial u_i}{\partial t}+u_i\frac{\partial u_i}{\partial x}=-\frac{e}{m_i}\frac{\partial V}{\partial x}-\nu_m u_i, \tag{2}$$

where $m_i$ is ion mass and $e$ is the electronic charge. In Eq. (2), $\nu_m=u_iN\sigma_t(u_i)$ is the total collision frequency for momentum loss, where $N$ is the neutral gas density, $\sigma_t(u_i)$ is the total collision cross section [22,23]. The electric potential inside the sheath is governed by the Poisson equation

$$\frac{\partial^2 V}{\partial x^2}=-\frac{e}{\varepsilon_0}(n_i-n_e), \tag{3}$$

where the electric potential, $V(x,t)$, is related the sheath electric field, $E(x,t)$, by $E(x,t)=-\partial V(x,t)/\partial x$. Here $\varepsilon_0$ is the permittivity of free space and $n_e(x,t)$ is the electron density. In a previous sheath model [14–16], the time-derivative terms in Eqs. (1) and (2) are omitted and the potential $V(x,t)$ in Eq. (2) is replaced by a time-averaged potential, which is valid at high frequencies. In the present model, we retain all the time-dependent terms in the ion fluid equations, so that the model is valid over a wide bias frequency range.

Due to the electron plasma frequency $\omega_{pe}$ being much higher than the rf frequency $\omega$, we can assume that the electrons are inertialess and respond to the instantaneous electric field. In contrast to the step model [14–16], here we consider that the electron density in the sheath changes continuously and is given by the Boltzmann distribution

$$n_e(x,t)=n_0\exp\left(\frac{eV(x,t)}{k_BT_e}\right), \tag{4}$$

where $n_0$ is the plasma density, $T_e$ is the electron temperature, and $k_B$ is the Boltzmann constant.

It is necessary to choose the appropriate boundary conditions before solving Eqs. (1)–(3). According to Riemann's theory [24], the Bohm criterion is not valid for the collisional sheath boundary. In this case, one should consider the existence of a presheath region between the bulk plasma and the sheath. At the presheath-plasma boundary, $x=d_p$, the ion density should be equal to the bulk plasma density,

$$n_i(d_p,t)=n_0, \tag{5}$$

and ions coming from the bulk plasma enter the presheath with a velocity equal to zero, i.e.,

$$u_i(d_p,t)=0. \tag{6}$$

In addition, the potential at the boundary is assumed as zero, i.e.,

$$V(d_p,t)=0. \tag{7}$$

On the other hand, at the sheath-presheath boundary, $x=d_s(t)$, we assume that the ion density is equal to the electron density, i.e., the quasineutral condition,

$$n_i(d_s,t)=n_e(d_s,t). \tag{8}$$

Here we should stress that, in contrast to the presheath-plasma boundary, the sheath-presheath boundary is instantaneous in the time.

Finally, we assume that at the electrode $(x=0)$ the potential is equal to an instantaneous voltage, i.e.,

$$V(0,t)=V_e(t). \tag{9}$$

It is well known that the instantaneous voltage depends on not only the applied rf power, but also instantaneous characteristics of the sheath itself. The relationship between the instantaneous voltage $V_e(t)$ and the instantaneous sheath thickness $d_s(t)$ can be determined self-consistently by the equivalent circuit model [10]

$$I_i(t)-I_e(t)-I_d(t)=I_{\max}\sin(2\pi ft). \tag{10}$$

Here, the first two terms on the left-hand side are the ion current and the electron current incident on the electrode, respectively, and the third term is the capacitive displacement current due to temporal variation of the voltage at the electrode, whereas the term on the right-hand side is the applied rf-bias current with the amplitude $I_{\max}$ and the frequency $f$. The expressions of $I_i(t)$, $I_e(t)$, and $I_d(t)$ can be found in Ref. [10].

Now we get a set of closed nonlinear equations that determines the spatiotemporal dependence of the collisional

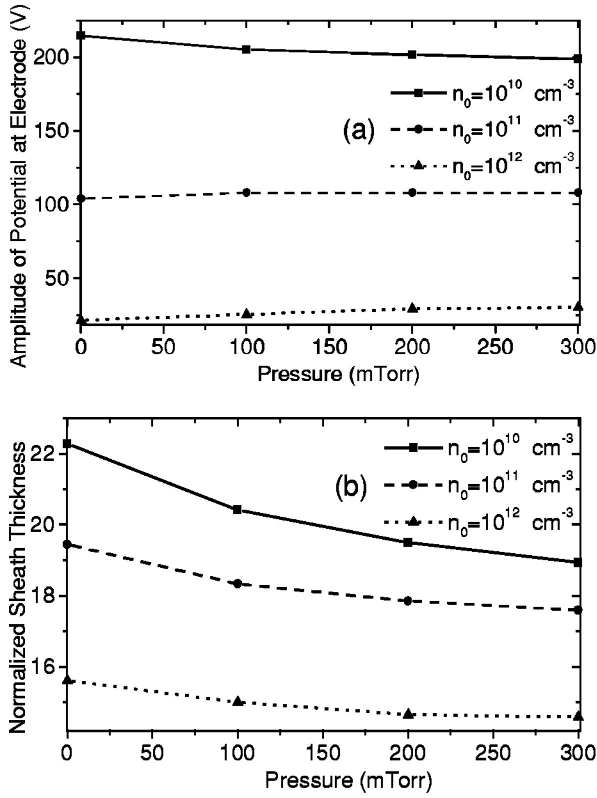


FIG. 1. The dependence of (a) the amplitude of the potential at the electrode and (b) the average sheath thickness on the pressure for different plasma densities. All the graphs have the same rf-bias power $P=50$ W, bias frequency $f=13.56$ MHz, and electron temperature $k_BT_e=3$ eV.

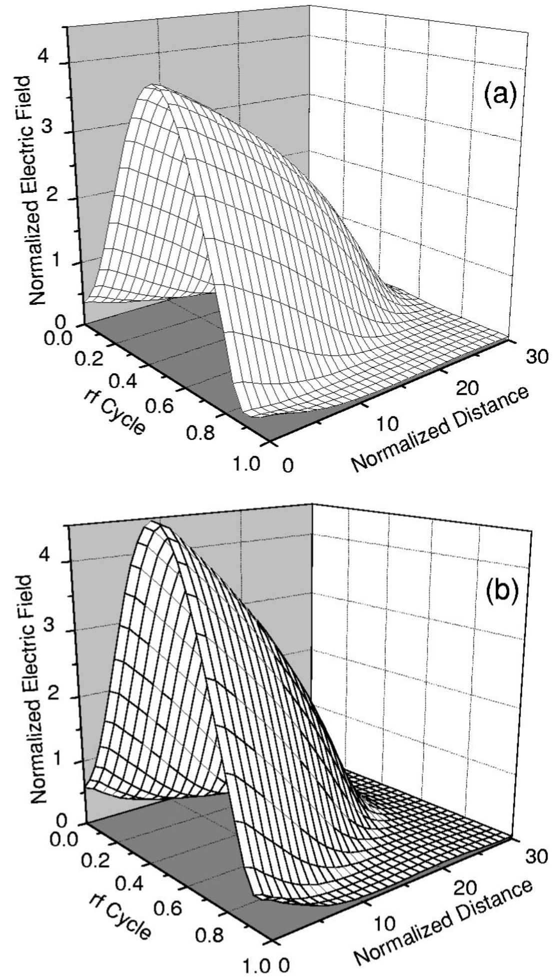


FIG. 2. The spatiotemporal profiles of the sheath electric field for (a) the collisionless case and (b) a discharge pressure 300 mTorr. The plasma density is $1.0\times10^{10}$ cm$^{-3}$, and other input parameters are the same as those used in Fig. 1.

rf sheath. The above equations with the boundary conditions will be solved numerically by using a finite difference scheme with an iterative process [10]. In the following simulations, we take an argon discharge as an example in which all the base values of the input parameters, such as $k_BT_e=3$ eV, $f=13.56$ MHz, and $A=325$ cm$^2$ (the electrode area). The amplitude $I_{\max}$ of the rf-bias current can be fixed by the rf-bias power as follows:

$$P=\frac{1}{\tau}\int_0^\tau dt\, I_{\max}\sin(2\pi ft)V_e(t), \tag{11}$$

where $\tau=1/f$ is the rf cycle. Furthermore, for convenience in calculations, we use the Debye length $\lambda_d$, the ion plasma frequency $\omega_{pi}$, the Bohm velocity $u_B$, the plasma density $n_0$, and the electron temperature $k_BT_e/e$ to nondimensionalize the position $x$, the time $t$, the ion velocity $u_i$, the ion density $n_i$, and the potential $V$, respectively.

Figure 1 shows the effects of the pressure on (a) the amplitude of potential at the electrode and (b) the average sheath thickness for the same power value, 50 W. It is clear that, as the pressure is increased, the amplitude of the potential decreases in the low-density case, while the amplitude of the potential increases slightly in the high-density case. The results illustrate that, if keeping the rf-bias power constant, the collisional effects play different roles in variations of the potential at the electrode for the different plasma densities. Meanwhile, we observe that, whether for the low or high plasma density, the average sheath thickness decreases as the pressure increases.

We show in Fig. 2 that the spatiotemporal profiles of the sheath electric field for (a) the collisionless case and (b) a given pressure $p=300$ mTorr. We notice from the figures that the collisional effects influence the spatiotemporal variation of the electric field inside the sheath. Also, the electric field oscillates fast in a rf cycle and decreases with an increasing distance from the electrode. Therefore, we may expect that the collisional effects on the electric field will affect the ion transport in the sheath.

## III. ION ENERGY AND ANGULAR DISTRIBUTIONS

In this section, with the spatiotemporal variation of the electric field obtained in Sec. II, we simulate the ion transport across the presheath and sheath by the Monte Carlo method and further determine the IEDs and IADs impinging

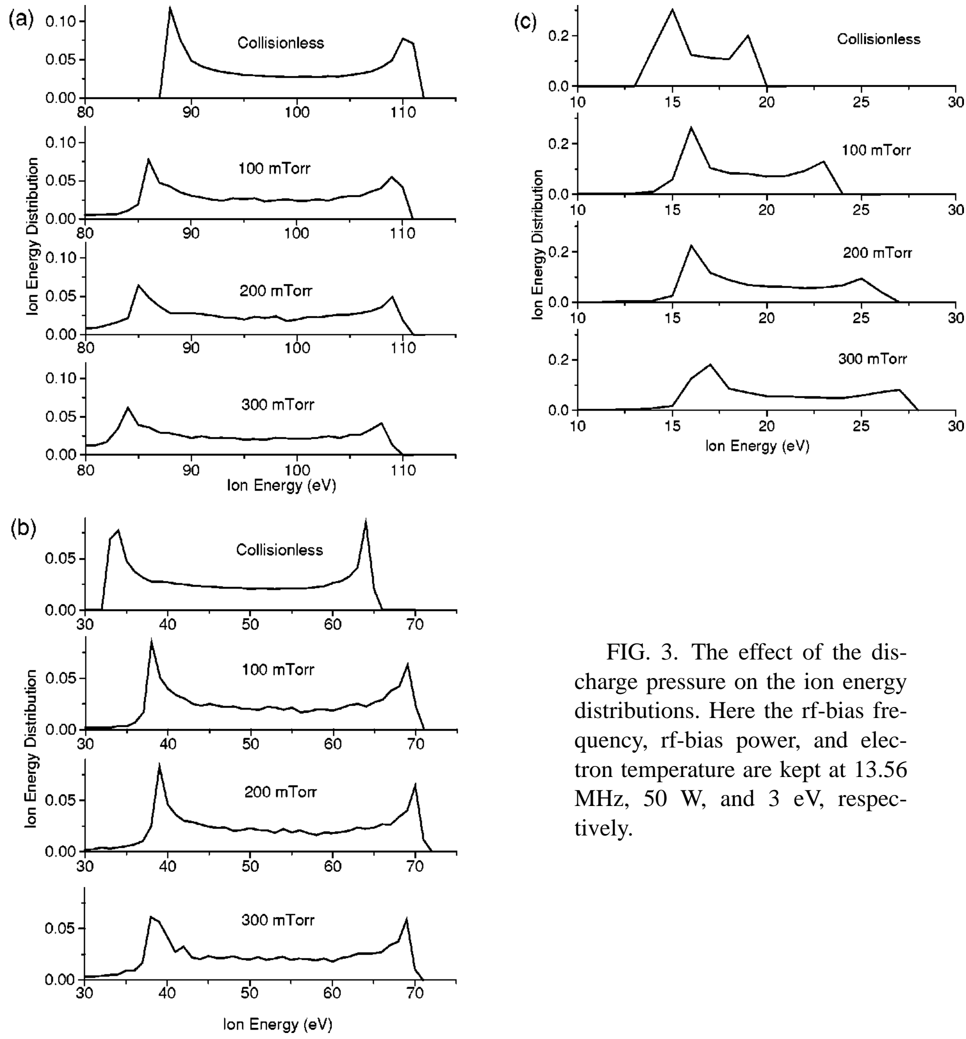


FIG. 3. The effect of the discharge pressure on the ion energy distributions. Here the rf-bias frequency, rf-bias power, and electron temperature are kept at 13.56 MHz, 50 W, and 3 eV, respectively.

on the electrode. For the collisionless sheath, an ion is accelerated only by the electric field and its trajectory is a line normal to the electrode surface. For the collisional sheath, besides the electric field acceleration, the ion will collide frequently with neutrals, which results in momentum and energy transfer. Thus, one may expect that ion-neutral collisions in the sheath can alter the IEDs and IADs from the collisionless case.

Assume that the ion enters the presheath from the bulk plasma, with an initial velocity which is picked randomly from a Boltzmann velocity distribution with temperature $T_i$, where $T_i = 580$ K. The motion for the ions due to the electric field acceleration is determined by the equation

$$m_i \frac{d^2x(t)}{dt^2} = eE(x,t). \tag{12}$$

Here the electric field is calculated from the simultaneous solution of the sheath model.

In order to model collisions, we consider the two major collisional processes between ions and neutrals, i.e., the charge-exchange collisions and elastic collisions. Each of these processes has its own collision cross section which is dependent upon the energy. For elastic scattering, the hard sphere model is adopted:

$$\varepsilon_1 = \varepsilon \cos^2(\theta_c/2), \tag{13}$$

where $\varepsilon_1$ and $\varepsilon$ are the energy of the incident and scattered ion, respectively. The scattering angle $\theta_c$ in the center of mass can be obtained by

$$\theta_c = \cos^{-1}(1 - 2\xi_1), \tag{14}$$

where $\xi_1$ is a random number from 0 to 1. According to the theory of the elastic two-body collision, the scattering angle $\theta_r$ in the laboratory can be written as

$$\tan \theta_r = \sin \theta_c / (1 + \cos \theta_c). \tag{15}$$

Thus, the deflection angle of the ion velocity after the $i$th collision is determined by the formula

$$\cos \varphi^{(i)} = \cos \varphi^{(i-1)} \cos \theta_r^{(i)} + \sin \varphi^{(i-1)} \sin \theta_r^{(i)} \sin \Psi^{(i)}. \tag{16}$$

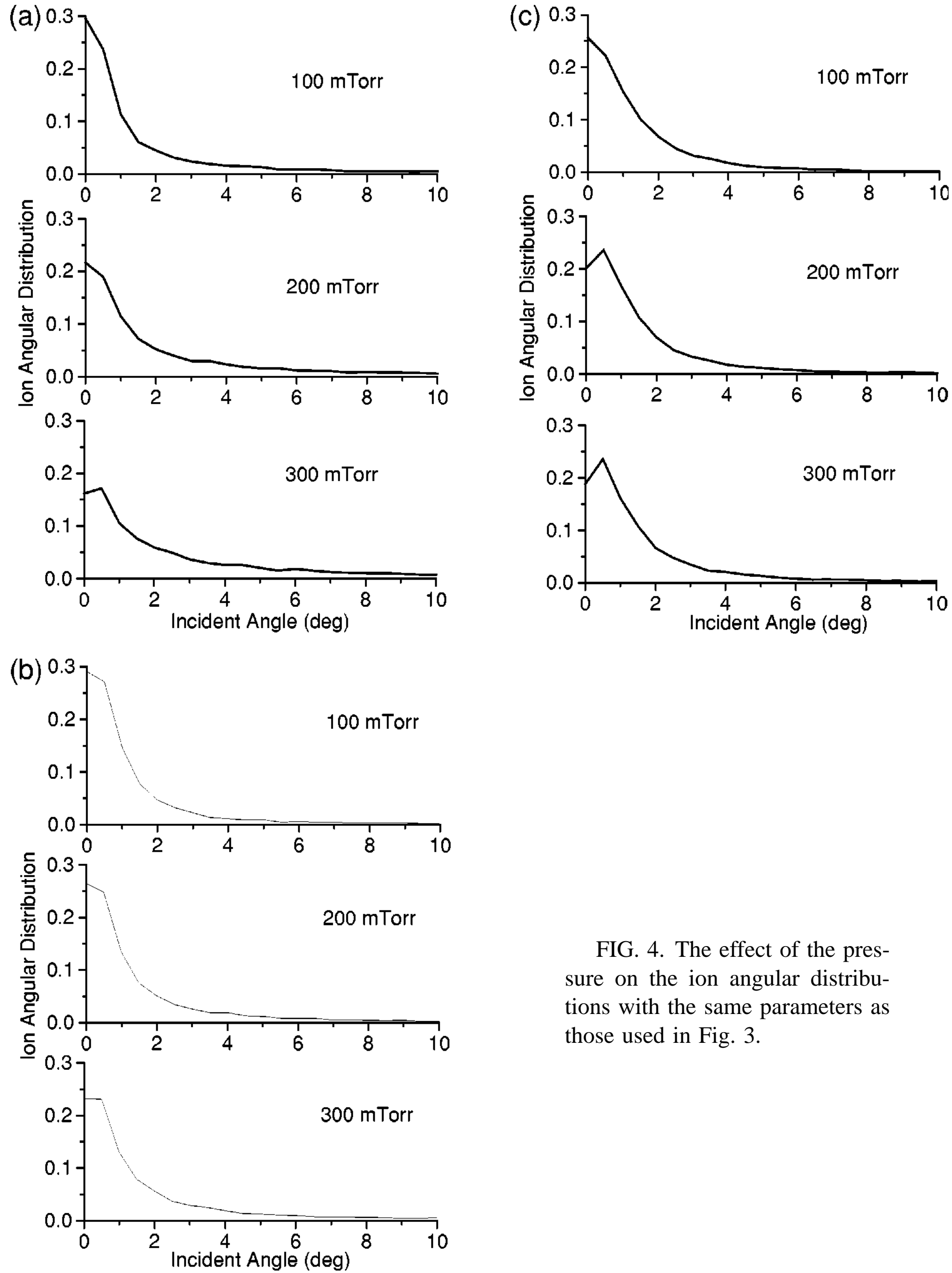


FIG. 4. The effect of the pressure on the ion angular distributions with the same parameters as those used in Fig. 3.

where $\Psi=2\pi\xi_2$ is the azimuthal angle of the ion velocity and $\xi_2$ is also a random number from 0 to 1.

For the charge-exchange collisions, as the fast ion closes to an Ar atom, an electron from the atom transfers to the ion, neutralizing it. After the interaction the original ion which is now an Ar atom continues along its previous trajectory but will no longer experience any acceleration under the electric field, while the original atom now becomes an ion with an initial velocity chosen randomly from a Maxwellian distribution. The scattering and azimuthal angles for the new ion can be randomly determined,

$$\theta_c=2\pi\xi_3, \quad \Psi=2\pi\xi_4, \tag{17}$$

where $\xi_3$ and $\xi_4$ are two random numbers (between 0 and 1).

In the simulation, the cross sections for the elastic (*el*) scattering and the charge-exchange (*cx*) collisions between $Ar^+$ and Ar are shown as follows [22,23]:

$$\sigma_{el}=40.04(1.0-0.0563\ln\varepsilon)^2 \tag{18}$$

and

$$\sigma_{cx}=47.05(1.0-0.0557\ln\varepsilon)^2, \tag{19}$$

where cross sections are in $10^{-16}$ cm$^2$ and the ion kinetic energy, $\varepsilon$ in eV. Thus, the total cross section is given by

$$\sigma_t(\varepsilon)=\sigma_{el}(\varepsilon)+\sigma_{cx}(\varepsilon). \tag{20}$$

By solving Eq. (12), one can get the ion passage distance $\Delta x$ in the sheath during the time interval $\Delta t$. Ions will suffer either an elastic collision or a charge-exchange collision when the passage distance $\Delta x$ is smaller than the distance between collisions, $l = -\lambda \ln \xi_5$, where $\lambda = 1/(N\sigma_t)$ is the mean free path and $\xi_5$ is a random number (between 0 and 1). The collisional type is randomly determined by $\sigma_{el}/\sigma_t$ and $\sigma_{cx}/\sigma_t$. After the collision, one can calculate the ion's trajectory and the new velocity. This process is continued until the ion strikes the electrode. At this point, we store its energy and angle of incidence. We use typically $10^4$ ion trajectories to obtain the IEDs and IADs with a reasonable signal-to-noise level. The input parameters in the following simulations are the same as those used in the last section.

Figure 3 shows the collisional effects on the IEDs versus discharge pressures for different plasma densities. At low pressures, a significant number of ions experience no collisions when crossing the sheath. As the pressure is increased, however, due to the ions going through a great deal of charge-exchange collisions, the heights of both peaks decrease, especially for the high-energy peaks. Also, as the pressure increases, the location of the high energy peak decreases at the low plasma density, while it increases at the high plasma density. The reason for this is that the location of the high energy peak depends on the amplitude of voltage at the electrode; see Fig. 1.

Finally, collisional effects on the IADs are shown in Fig. 4 for different discharge pressures and different plasma densities. As the discharge pressure increases, the IADs spread to large angle regions, which results from the ions undergoing a number of collisions with neutrals in the sheath. The spreading in angle of the IADs has important consequences in plasma etching, where an anisotropic delivery of activation energy to the surface is required to obtain vertical etches. Therefore, one can see that the plasma density and the sheath electric field (or the amplitude of voltage) as well as the collision effects are crucial factors in determining the form of the IEDs and IADs.

## IV. CONCLUSIONS

In this paper, we have used a hybrid theoretical model to study the characteristics of a rf sheath and the IEDs and IADs on a rf-biased electrode. A one-dimensional dynamical model of a collisional rf sheath has been developed to determine the influence of the discharge pressure on the spatial distributions of some physical quantities in the sheath, such as the amplitude of voltage at the electrode, the average sheath thickness, and the spatiotemporal variation of the electric field inside the sheath. The Monte Carlo method has been used to predict the energy distributions and angular distributions of ions impinging on a rf-biased electrode. It has been shown from the numerical results that both the plasma density and the discharge pressure affect significantly the amplitude of the potential on the electrode and the sheath thickness. In other words, the plasma density and the discharge pressure affect the characteristics of the rf sheath, and further, affect the IEDs and IADs on the electrode. In the future work, we will extend the present model to study the effects of the active particles on the characteristics of the rf sheath.

## ACKNOWLEDGMENT

This work was jointly supported by the National Natural Science Foundation of China (Grant No. 19975008) and the Grant for Striding-Century Excellent Scholar of Ministry of Education State of China.

[1] M.A. Lieberman, IEEE Trans. Plasma Sci. **16**, 638 (1988).
[2] V.A. Godyak and N. Sternberg, Phys. Rev. A **42**, 2299 (1990).
[3] M.A. Sobolewski, Phys. Rev. E **56**, 1001 (1997).
[4] J. Gierling and K.-U. Riemann, J. Appl. Phys. **83**, 3521 (1998).
[5] E.A. Edelberg and E.S. Aydil, J. Appl. Phys. **86**, 4799 (1999).
[6] P.A. Miller and M.E. Riley, J. Appl. Phys. **82**, 3689 (1997).
[7] D. Bose, T.R. Govindan, and M. Meyyappan, J. Appl. Phys. **87**, 7176 (2000).
[8] M.A. Sobolewski, Phys. Rev. E **62**, 8540 (2000).
[9] V. Midha and D.J. Economou, J. Appl. Phys. **90**, 1102 (2001).
[10] Z.L. Dai, Y.N. Wang, and T.C. Ma, Phys. Rev. E **65**, 036403 (2002).
[11] E.A. Edelberg, A. Perry, N. Benjamin, and E.S. Aydil, J. Vac. Sci. Technol. A **17**, 506 (1999).
[12] J.R. Woodworth, I.C. Abraham, M.E. Riley, P.A. Miller, T.W. Hamilton, B.P. Argon, R.J. Shul, and C.G. Willison, J. Vac. Sci. Technol. A **20**, 873 (2002).
[13] I.C. Abraham, J.R. Woodworth, M.E. Riley, P.A. Miller, T.W. Hamilton, and B.P. Argon, J. Vac. Sci. Technol. A **20**, 1759 (2002).
[14] M.A. Lieberman, IEEE Trans. Plasma Sci. **17**, 338 (1989).
[15] K. Böring, Appl. Phys. Lett. **60**, 1553 (1992).
[16] H.T. Qin, Y.N. Wang, and T.C. Ma, J. Appl. Phys. **90**, 5884 (2001).
[17] M.J. Kushner, J. Appl. Phys. **58**, 4024 (1985).
[18] B.E. Thompson, H.H. Sawin, and D.A. Fisher, J. Appl. Phys. **63**, 2241 (1988).
[19] J. Liu, G.L. Huppert, and H.H. Sawin, J. Appl. Phys. **68**, 3916 (1990).
[20] P.W. May, D. Field, and D.F. Klemperer, J. Appl. Phys. **71**, 3721 (1992).
[21] H.T. Qiu, Y.N. Wang, and T.C. Ma, Acta Physica Sinica **51**, 1332 (2002).
[22] M.A. Lieberman, and A.J. Lichtenberg, in *Principles of Plasma Discharges and Materials Processing* (Wiley, New York, 1994), p. 137.
[23] D. Kim and D.J. Economou, IEEE Trans. Plasma Sci. **30**, 2048 (2002).
[24] K.-U. Riemann, Phys. Plasmas **4**, 4158 (1997).